BJP British Journal of Pharmacology

DOI:10.1111/bph.12834
www.brjpharmacol.org

RESEARCH PAPER

Treatment with LPS plus INF-γ induces the expression and function of muscarinic acetylcholine receptors, modulating NIH3T3 cell proliferation: participation of NOS and COX

A J Español, M O Maddaleno, M G Lombardi, M Cella, P Martínez Pulido and M E Sales

Facultad de Medicina, Universidad de Buenos Aires, Centro de Estudios Farmacológicos y Botánicos (CEFYBO)-CONICET, Buenos Aires, Argentina

Correspondence
Professor Maria Elena Sales, 2da Cátedra de Farmacología Facultad de Medicina, UBA, Centro de Estudios Farmacológicos y Botánicos-CONICET, Paraguay 2155 piso 16 CABA, Buenos Aires CP 1121, Argentina. E-mail malegazpio@yahoo.com.ar

Received
13 November 2013
Revised
17 June 2014
Accepted
24 June 2014

BACKGROUND AND PURPOSE

LPS and IFN-γ are potent stimuli of inflammation, a process in which fibroblasts are frequently involved. We analysed the effect of treatment with LPS plus IFN-γ on the expression and function of muscarinic acetylcholine receptors in NIH3T3 fibroblasts with regards to proliferation of these cells. We also investigated the participation of NOS and COX, and the role of NF-κB in this process.

EXPERIMENTAL APPROACH

NIH3T3 cells were treated with LPS (10 ng·mL^{-1}) plus IFN-γ (0.5 ng·mL^{-1}) for 72 h (iNIH3T3 cells). Cell proliferation was evaluated with MTT and protein expression by Western blot analysis. NOS and COX activities were measured by the Griess method and radioimmunoassay respectively.

KEY RESULTS

The cholinoceptor agonist carbachol was more effective at stimulating proliferation in iNIH3T3 than in NIH3T3 cells, probably due to the *de novo* induction of M_3 and M_5 muscarinic receptors independently of NF-κB activation. iNIH3T3 cells produced higher amounts of NO and PGE_2 than NIH3T3 cells, concomitantly with an up-regulation of NOS1 and COX-2, and with the *de novo* induction of NOS2/3 in inflamed cells. We also found a positive feedback between NOS and COX that could potentiate inflammation.

CONCLUSIONS AND IMPLICATIONS

Inflammation induced the expression of muscarinic receptors and, therefore,stimulated carbachol-induced proliferation of fibroblasts. Inflammation also up-regulated the expression of NOS and COX-2, thus potentiating the effect of carbachol on NO and PGE_2 production. A positive crosstalk between NOS and COX triggered by carbachol in inflamed cells points to muscarinic receptors as potential therapeutic targets in inflammation.

Abbreviations

nNCS, non-neuronal cholinergic system

Table of Links

TARGETS	LIGANDS
COX-1	Aminoguanidine
COX-2	Atropine
Cytokine receptors	cAMP
M_1 receptor	Carbachol
M_2 receptor	4-DAMP
M_3 receptor	IFN-γ
M_4 receptor	Indomethacin
M_5 receptor	LPS
Nicotinic receptors	Mecamylamine
NOS1 (neuronal NOS)	Methoctramine
NOS2 (inducible NOS)	NO
NOS3 (endothelial NOS)	PGE_2
PLA_2	Pilocarpine
	Pirenzepine
	Tropicamide
	Xanomeline

This Table lists key protein targets and ligands in this document, which are hyperlinked to corresponding entries in http://www.guidetopharmacology.org, the common portal for data from the IUPHAR/BPS Guide to PHARMACOLOGY (Pawson *et al.*, 2014) and are permanently archived in the Concise Guide to PHARMACOLOGY 2013/14 (Alexander *et al.*, 2013a,b,c,d).

Introduction

Inflammation, a highly regulated response to infection and injury, has evolved as a beneficial component of the physiological defence system of the host organism. Inflammatory processes are identified as acute and chronic inflammation according to their duration. Acute inflammation has a rapid onset and short duration and presents exudation of fluid and plasma proteins, in addition to migration of leukocytes and neutrophils. Chronic inflammation has a longer duration and is associated with the presence of macrophages, lymphocytes, blood vessel proliferation, fibrosis and tissue necrosis. This type of inflammatory process can progress to an asymptomatic response that causes tissue damage in various diseases such as rheumatoid arthritis, diabetes, atherosclerosis and cancer (Kumar and Chakrabarti, 2009). One of the most important causes of inflammation is bacterial infection. For this reason, inflammation can be induced by administering bacterial LPS, which is the main constituent of the outer membrane of Gram-negative bacteria, or by combining LPS with inflammatory cytokines such as IFN-γ, which acts synergistically to up-regulate gene expression in different cell types. However, some features of the inflammatory response remain unique or 'private' to the tissue where inflammation occurs. The molecular and cellular basis for such tissue tropism has remained elusive. There is now accumulating evidence that fibroblasts help define tissue topography, provide positional memory and regulate the switch from acute to chronic inflammation. Fibroblasts are active promoters of tissue formation and tissue remodelling; they actively define the structure of the tissue microenvironment and modulate immune cell behaviour by conditioning the local cellular and cytokine microenvironment so that the kinetics and nature of the inflammatory infiltrate are appropriate to the cause of the damage (Buckley, 2003).

Recently, it has been documented that components of the non-neuronal cholinergic system (nNCS) such as acetylcholine and choline acetyl transferase are expressed in human fibroblasts derived from the loose connective tissue (Spang *et al.*, 2013), and it is known that the nNCS is widely involved in inflammatory responses (Forsgren *et al.*, 2009). Muscarinic acetylcholine receptors are components of the nNCS and molecular cloning has identified five subtypes. M_1, M_3 and M_5 receptor subtypes are classically coupled to $G_{q/11}$ protein, triggering phospholipase C/NOS, or to phospholipase A_2/COX metabolic pathway activity (Kohn *et al.*, 1996), while M_2 and M_4 receptors inhibit cAMP accumulation via Gi/o protein (Eglen, 2012). The aims of this work were to investigate the role of muscarinic acetylcholine receptors in cell proliferation and to characterize muscarinic acetylcholine receptor expression in NIH3T3 murine fibroblasts under inflammatory conditions induced by LPS plus IFN-γ treatment. We also analysed the expression and function of NOS and COX as effector enzymes of muscarinic acetylcholine receptor activation and the role of NF-κB in this process.

Methods

Cell culture

The normal murine fibroblast cell line NIH3T3 (CRL-1658) (ATCC, Manassas, VA, USA) was cultured in DMEM : F12 (1:1)

(Invitrogen, Buenos Aires, Argentina) with 2 mM L-glutamine, 80 μg·mL^{-1} gentamicin supplemented with 10% heat-inactivated fetal calf serum (FCS) (Bioser S.A., Barcelona, Spain) at 37°C in a humidified 5% CO_2 air. Cells were detached using 0.25% trypsin and 0.02% EDTA in Ca^{2+}- and Mg^{2+}-free PBS of confluent monolayers. Medium was replaced three times a week. Cell viability was assayed by the Trypan blue exclusion test. Hoechst staining confirmed the absence of mycoplasma (Chen, 1977).

NIH3T3 cells were treated with 10 ng·mL^{-1} LPS from *Escherichia coli* 026:B6 and 0.5 ng·mL^{-1} IFN-γ for 72 h (iNIH3T3) in order to simulate a long-lasting inflammatory response. To induce quiescence, cells were deprived of FCS 24 h before any assay.

Cell proliferation assay

Proliferation was evaluated by using the soluble tetrazolium salt 3-(4,5-dimethylthiazol-2-yl)-2,5-diphenyltetrazolium bromide (MTT) colorimetric assay (Life Technologies, Eugene, OR, USA). In living cells, MTT is reduced to formazan. Cells were seeded in 96-well plates at a density of 10^4 cells per well in DMEM : F12 supplemented with 5% FCS and then left to adhere overnight. Subconfluent conditions of about 50–60% were chosen to allow detection of maximal growth. After being stimulated with LPS plus IFN-γ, cells were treated with increasing concentrations of the synthetic cholinoceptor agonist carbachol in triplicate for 1 h in the absence or presence of the non-selective muscarinic receptor antagonist atropine (10^{-8} M), or the nicotinic receptor antagonist mecamylamine (10^{-8} M), or the selective antagonists pirenzepine for M_1 receptors, methoctramine for M_2 receptors, 4-diphenylacetoxy-N-methyl-piperidine (4-DAMP) for M_3 receptors, tropicamide for M_4 receptors or xanomeline for M_5 receptors, all of them at 10^{-9} M, or the following different enzymatic inhibitors: A5727 (5×10^{-6} M), a NOS1 selective inhibitor, aminoguanidine (10^{-4} M), a NOS2 selective inhibitor, LN5-(1-iminoethyl) ornithine hydrochloride (I134) (10^{-5} M), a NOS3 selective inhibitor, indomethacin (10^{-6} M), a COX inhibitor, N-[2-(cyclohexyloxy)-4-nitrophenyl] methane-sulfonamide (NS398) (10^{-5} M), a COX-2 selective inhibitor, or N-(3,5-bistrifluoromethylphenyl)-5-chloro-2-hydroxybenzamide (IMD354) (10^{-6} M), a NF-κB inhibitor, which were added to carbachol 30 min previously. After treatment, the medium was replaced by fresh medium free of FCS and cells were cultured for 24 h. Supernatants were discarded, and viable cells were detected by adding 110 μL of MTT solution prepared by diluting 10 μL of 5 mg·mL^{-1} MTT in PBS, in 100 μL medium free of phenol red and FCS to each well. After incubation for 4 h at 37°C, the production of formazan was evaluated by measuring the absorbance at 540 nm with an ELISA reader (BioTek, Winooski, VT, USA). Values are mean ± SEM and results are expressed as % stimulation with respect to control (considered as 100%).

Detection of muscarinic acetylcholine receptors by Western blot

Cells (2×10^6) were washed twice with PBS and lysed in 1 mL of 50 mM Tris-HCl, 50 mM NaCl, 5 mM NaF, 5 mM $MgCl_2$, 1 mM EDTA, 1 mM EGTA, 5 mM PMSF, 1% Triton X-100 and 10 μg·mL^{-1} trypsin inhibitor, aprotinin and leupeptin, pH 7.4. After 1 h in an ice bath, lysates were sonicated for 30 s at 4°C and centrifuged at 8000× *g* for 20 min at 4°C. The supernatants were stored at –80°C and protein concentration was determined by the method of Bradford (1976). Samples (80 μg protein per lane) were subjected to 10% SDS-PAGE minigel electrophoresis, transferred to nitrocellulose membranes, and incubated overnight with goat anti-mouse M_1, M_2 or M_3 receptor polyclonal antibodies or rabbit anti-mouse M_4 or M_5 receptor polyclonal antibodies, all diluted 1:100 (Santa Cruz Biotechnology Inc., Dallas, TX, USA) (Español and Sales, 2004). Then strips were incubated with HRP-linked anti-rabbit IgG or anti-goat IgG, both diluted 1:10 000 in 20 mM Tris-HCl buffer, 150 mM NaCl and 0.05% Tween 20 (TBS-T) at 37°C for 1 h. Bands were visualized by electrochemiluminescence (ECL). Densitometric analysis of the bands is expressed as optical density units relative to the expression of GAPDH.

Transfection of NIH3T3 cells with small interference RNA to muscarinic acetylcholine receptors

A double-stranded siRNA targeting M_3 receptor subtype was designed in our laboratory. The extension of M_3-siRNA was a 21-nucleotide duplex, and its sequences were 5-GUGGUC UUCAUCGCUUUCUUA-3 and 5-AGAAAGCGAUGAAGAC CACUU-3 corresponding to positions 981–1002 relative to the start codon (Life Technologies). To down-regulate M_5 receptor expression, the siRNA duplex was purchased from Life Technologies (Cat No. 4390771, ID s102952; Ambion, Eugene, TX, USA). To perform transfection, NIH3T3 cells (10^6 cells in 0.2 mL) were electroporated with or without 1 μg of M_3 or M_5-siRNA. Electroporation was performed in a 4 mm gap cuvette using the Gene pulser XCell device (BioRad, Oakland, CA, USA) with the following conditions: 50 V and 1000 μF of capacitance. Immediately after electroporation, cells were suspended in complete medium and left to recover. After 3 h, cells were treated with LPS plus INF-γ as stated previously. We confirmed the effectiveness of siRNA transfection by Western blot. iNIH3T3 cells transfected with M_3 or M_5-siRNA were used in the proliferation, NO and PGE_2 assays.

NO production

NO production was quantified by measuring nitrite (NO_2^-) accumulation in cell culture supernatants. Cells (10^4 per well) were seeded in triplicate in 96-well plates with 100 μL DMEM : F12 supplemented with 10% FCS. After being deprived of FCS (starvation), cells were treated with different concentrations of carbachol in triplicate for 1 h in the absence or presence of the muscarinic antagonists atropine (10^{-8} M), pirenzepine, methoctramine, 4-DAMP, tropicamide or xanomeline, all of them at 10^{-9} M, or different enzymatic inhibitors: A5727 (5×10^{-6} M), aminoguanidine (10^{-4} M), I134 (10^{-5} M), indomethacin (10^{-6} M), NS398 (10^{-5} M) or IMD354 (10^{-6} M). The antagonists or enzymatic inhibitors were added 30 min before carbachol. Then culture medium was replaced by fresh medium free of phenol red and FCS. NO_2^- accumulation was evaluated after 24 h in culture supernatants by Griess reagent [1% sulphanylamine in 30% acetic acid with 0.1% N-(1 naphtyl) ethylenediamine in 60% acetic acid]. Absorbance was measured at 540 nm with an ELISA Reader (BioTek). The concentration of NO_2^- in samples was

obtained by extrapolation from a standard curve of $NaNO_2$ diluted in culture medium. Results are expressed as μM concentration of NO_2^- in culture supernatants.

Detection of NOS isoforms by Western blot

Cells (2×10^6) were washed twice with PBS and lysed in 1 mL of modified RIPA buffer: 50 mM Tris-HCl; 150 mM NaCl; 1 mM NaF, EDTA and PMSF; 1% Triton X-100; 4 μg·mL^{-1} trypsin inhibitor; 5 μg·mL^{-1} aprotinin; 5 μg·mL^{-1} leupeptin, pH 7.4. After 1 h in an ice bath, lysates were centrifuged at 8000× *g* for 20 min at 4°C (Fiszman *et al.*, 2006). Supernatants were stored at –80°C and the protein concentration was determined by the method of Bradford (1976).

Samples (80 μg protein per lane) were subjected to 7.5% SDS-PAGE minigel electrophoresis, transferred to nitrocellulose membranes, and incubated overnight with polyclonal antibodies anti-NOS1 or anti-NOS3 raised in rabbit or anti-NOS2 raised in goat, all diluted 1:100 (Santa Cruz Biotechnologies Inc.) in TBS-T (20 mM Tris-HCl buffer, 150 mM NaCl and 0.05% Tween 20). After several rinses with TBS-T, strips were incubated with anti-rabbit IgG conjugated with HRP, diluted 1:10 000 or anti-goat IgG conjugated with HRP, diluted 1:20 000 in TBS-T at 37°C for 1 h. ECL was used to visualize the bands that were quantified by densitometric analysis.

Quantification of PGE_2 levels by radioimmunoassay

Cells (10^6 per well) were incubated in 1 mL of DMEM : F12 at 37°C, treated with different concentrations of carbachol for 1 h in the absence or presence of atropine (10^{-8} M), or pirenzepine, methoctramine, 4-DAMP, tropicamide or xanomeline, all of them at 10^{-9} M, or different enzymatic inhibitors: A5727 (5×10^{-6} M), aminoguanidine (10^{-4} M), I134 (10^{-5} M), indomethacin (10^{-6} M), NS398 (10^{-5} M) or IMD354 (10^{-6} M). The antagonists or enzymatic inhibitors were added to carbachol 30 min before. Then medium was replaced by the same volume of fresh medium and PGE_2 production was determined by a radioimmunoassay procedure, according to a previously described method (Granstrom and Kindhal, 1978), after 90 min. Samples or standards (100 μL) were mixed with 500 μL of anti-rabbit PGE_2 antiserum (specific activity 154 Ci·mmol^{-1}; NEN Life Science Products Inc., Boston, MA, USA) added to each tube. All dilutions were prepared in 10 mM PBS, pH 7.4, containing 0.01% BSA and 0.1% sodium azide. After incubation, a dextran-coated charcoal suspension was added to separate bound and free fractions. The supernatants were removed from each tube and a scintillation cocktail was added to determine the amount of radioactivity. Results were expressed as ng·mL^{-1} of PGE_2 produced.

Detection of COX isoforms by Western blot

For the preparation of cell lysates and Western blot assays, we proceeded similarly to NOS immunodetection, but using anti-COX-1 or anti-COX-2 rabbit polyclonal antibodies (Cayman Chemical Co., Ann Harbor, MI, USA) diluted 1:150 in TBS-T. After several rinses with TBS-T, strips were incubated with anti-rabbit IgG conjugated with HRP, diluted 1:10 000 in TBS-T at 37°C for 1 h. The bands were visualized by ECL and quantified by densitometric analysis (Español *et al.*, 2007).

Drugs

Unless otherwise stated, all drugs were purchased from Sigma-Aldrich (St. Louis, MO, USA). Solutions were prepared fresh daily.

Statistics

Results are expressed as mean ± SEM of at least six experiments performed in duplicate or triplicate. When performed in duplicate or triplicate, these were used to determine accuracy of each $n = 1$. A GraphPad Prism computer programme (GraphPad Software, Inc., La Jolla, CA, USA) one-way ANOVA for paired samples was used to determine the significance of differences between mean values in all control and test samples. The analysis was complemented by using a Tukey test to compare the mean values. Differences between means were considered significant if $P < 0.05$.

Results

Effect of LPS plus IFN-γ on the effect of carbachol on the proliferation of NIH3T3 cells

We analysed the effect of carbachol on NIH3T3 cell proliferation after a long-lasting treatment with LPS plus IFN-γ. Figure 1A shows that carbachol stimulated iNIH3T3 cell proliferation in a concentration-dependent manner, with maximal effect 148 ± 5% and its maximal effective concentration (EC_{max}) 10^{-7} M. Similar results were observed in NIH3T3 cells; but carbachol (10^{-8} M) produced a lower maximal effect (134 ± 4%) than that in inflamed cells ($P < 0.05$). This effect of carbachol was significantly reduced by the pre-incubation of cells with the non-selective muscarinic antagonist atropine (106 ± 4% and 107 ± 6% for NIH3T3 and iNIH3T3, respectively), but not by mecamylamine, a nicotinic antagonist (136 ± 3% and 150 ± 6% for NIH3T3 and iNIH3T3 respectively). To analyse which subtypes of muscarinic acetylcholine receptors were involved in the proliferative action of the agonist, the EC_{max} was assayed in the presence of selective muscarinic antagonists for each experimental group (Figure 1B). Pirenzepine, methoctramine and tropicamide reduced the effects of carbachol on both cell populations. In contrast, 4-DAMP and xanomeline were effective at reducing carbachol-induced proliferation only in LPS plus IFN-γ-treated cells, thus revealing the participation of M_3 and M_5 receptor subtypes. To confirm differences in muscarinic acetylcholine receptor expression between the two experimental groups, we performed Western blot experiments in fibroblast lysates. iNIH3T3 cells showed not only the expression of M_1, M_2 and M_4 receptors but also *de novo* expression of M_3 and M_5 receptor subtypes (Figure 1C).

The expression of M_3 and M_5 receptors in iNIH3T3 cells was down-regulated by transfection with specific siRNAs targeting each receptor subtype, and Western blot experiments reveal a reduction in the amount of these proteins in cell lysates (Figure 2A). The latter was concomitant with a decrease in carbachol-induced iNIH3T3 cell proliferation (Figure 2B).

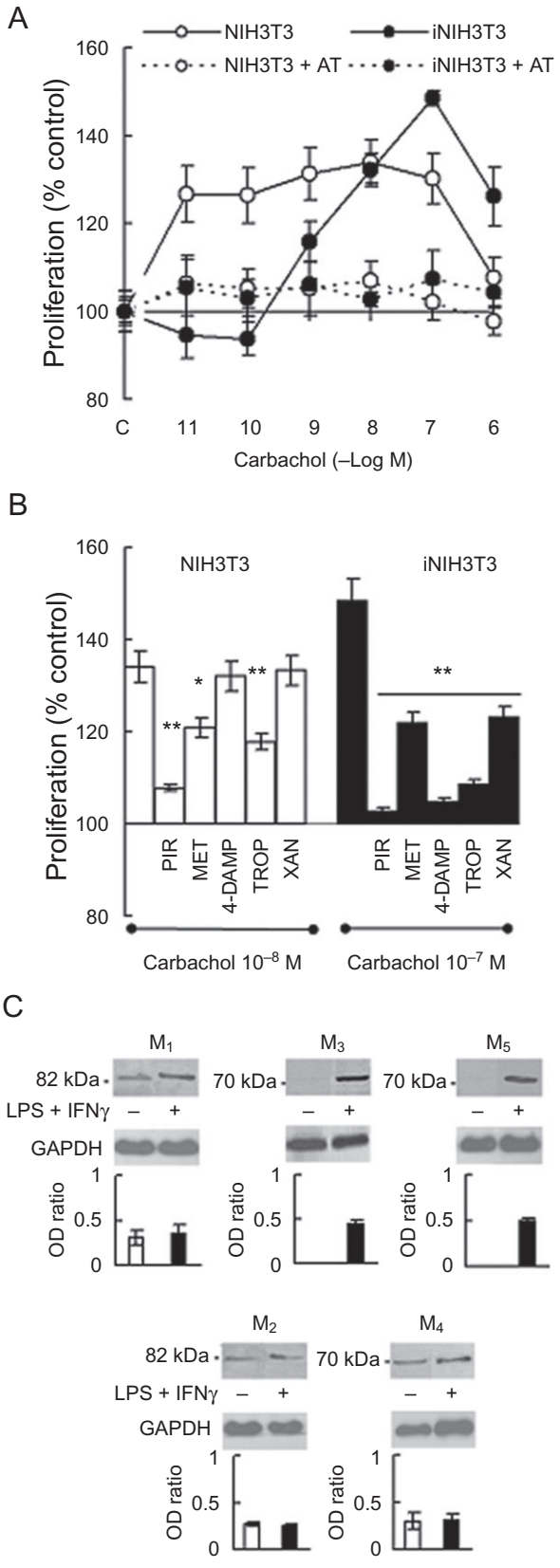

Figure 1

Activity and expression of muscarinic acetylcholine receptors in NIH3T3 cells. (A) Concentration–response curves for effect of carbachol on cell proliferation. Cells were cultured in the absence or presence of LPS (10 ng·mL^{-1}) plus IFN-γ (0.5 ng·mL^{-1}) for 72 h (NIH3T3 and iNIH3T3, respectively), and then stimulated with different concentrations of carbachol without or with atropine (AT) (10^{-8} M). (B) Effect of the maximal effective concentration of carbachol on cell proliferation in the absence or presence of 10^{-9} M pirenzepine (PIR), methoctramine (MET), 4-DAMP, tropicamide (TROP) or xanomeline (XAN). Results are expressed as % change with respect to control (considered as 100%). Values are mean ± SEM of six experiments performed in triplicate. *P < 0.01;**P < 0.001 versus carbachol. (C) Western blot assay to detect muscarinic acetylcholine receptor subtypes (M_1–M_5) in untreated or LPS plus IFN-γ-treated cells. Molecular weights are on the left. Densitometric analysis of the bands is expressed as optical density (OD) units relative to the expression of GAPDH protein used as loading control. One representative experiment of three is shown.

The involvement of NF-κB in the modulation of muscarinic acetylcholine receptor expression in NIH3T3 cells

As the induction of protein expression during inflammation may involve activation of the NF-κB pathway, we analysed the expression of muscarinic acetylcholine receptors in the presence of IMD354, which inhibits IκB kinase and prevents the translocation of NF-κB p65 to the nucleus. Western blot results revealed that IMD354 did not modify muscarinic receptor expression in either cell population (Figure 3).

Effect of LPS plus IFN-γ on muscarinic acetylcholine receptor function in NIH3T3 cells: participation of NOS-derived NO

As muscarinic acetylcholine receptor activation may lead to the stimulation of NOS-derived NO production, we analysed the effect of carbachol on NO synthesis in LPS plus IFN-γ-treated cells. This treatment increased the basal production of NO from 4.9 ± 0.5 μM to 8.4 ± 0.2 μM (P < 0.001). Carbachol induced a concentration–dependent effect on NO production in iNIH3T3 cells and the EC_{max} value was the same that inducing a maximal effect on proliferation. Atropine significantly reduced the action of carbachol (Figure 4A). In addition, the NO production in response to the EC_{max} of carbachol (10.7 ± 0.04 μM) was totally reduced by pirenzepine and 4-DAMP and partially inhibited by xanomeline in iNIH3T3 cells.

These results were confirmed by transfecting cells with siRNA targeting M_3 or M_5 receptors. Both siRNAs were equally potent to reduce carbachol-induced NO synthesis in iNIH3T3 cells (Figure 4B). In NIH3T3 cells, the effect of carbachol (7.8 ± 0.8 μM) appears to be mediated by the activation of M_2 and M_4 receptors and, to a lesser extent, by M_1 receptors, because methoctramine and tropicamide reduced carbachol-derived NO production in a more potent manner (P < 0.001) than pirenzepine (P < 0.05) (Figure 4B).

LPS plus IFN-γ treatment modified not only the coupling of muscarinic acetylcholine receptors to NO production, but also the expression of NOS isoforms as well, as NIH3T3 cells

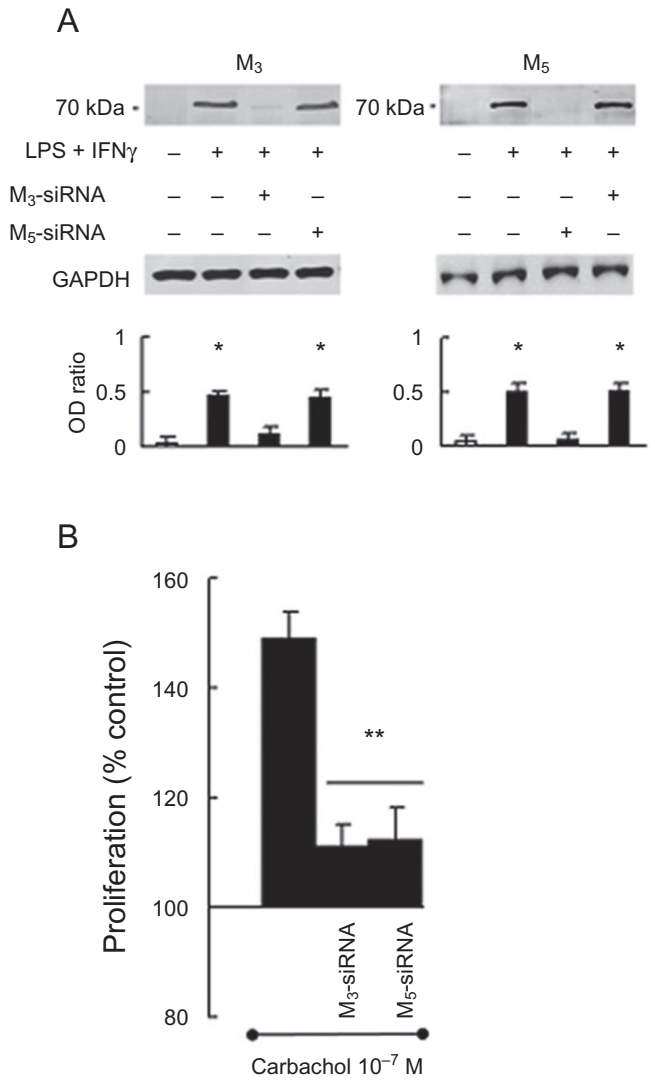

Figure 2

Participation of muscarinic receptor subtypes M_3 and M_5 in NIH3T3 cell proliferation. (A) Western blot assay to detect muscarinic acetylcholine receptor subtypes in LPS plus IFN-γ-treated cells in the absence or presence of M_3- or M_5-siRNA. Molecular weights are on the left. Densitometric analysis of the bands is expressed as optical density (OD) units relative to the expression of GAPDH protein used as loading control. One representative experiment of three is shown. *P < 0.01. (B) Action of the maximal effective concentration of carbachol (10^{-7}M) on iNIH3T3 cell proliferation in the absence or presence of M_3- or M_5-siRNA. Results are expressed as % change with respect to control (considered as 100%). Values are mean ± SEM of six experiments performed in triplicate. **P < 0.001 versus carbachol.

only expressed NOS1 protein, while iNIH3T3 cells had an up-regulated expression of the NOS1 enzyme and also expressed *de novo* NOS2 and NOS3 isoforms (Figure 4C). In line with these results, carbachol-stimulated NO production was reduced only by the NOS1 inhibitor A5727 (P < 0.001 vs. carbachol) in NIH3T3 cells, while in iNIH3T3 cells, carbachol-induced NO production was reduced not only by A5727, but also by aminoguanidine and I1-34, NOS2 and NOS3 inhibitors respectively (P < 0.001 vs. carbachol) (Figure 4D).

The participation of the NF-κB pathway in NOS expression and function was analysed in the presence of IMD354 in both cell populations. This inhibitor not only reduced NO production (P < 0.001) and NOS1 and NOS2 expression in iNIH3T3 cells, but also down-regulated NO synthesis (P < 0.001) and NOS1 expression in untreated cells (Figure 5A and B). IMD354 treatment had no effect on NOS3 expression (Figure 5B).

Effect of LPS plus IFN-γ on muscarinic acetylcholine receptor function in NIH3T3 cells: participation of COX-derived PGE_2

As it is well known that muscarinic acetylcholine receptor activation can promote prostanoid metabolism via phospholipase A_2/COX activation, we analysed the effect of carbachol on the production of PGE_2, an important inflammatory mediator in both cell populations. The addition of LPS plus IFN-γ increased the basal production of PGE_2 (iNIH3T3:1.71 ± 0.26 ng·mL^{-1}) in relation to untreated cells (NIH3T3: 0.80 ± 0.15 ng·mL^{-1}) (P < 0.05). Carbachol increased PGE_2 production in both experimental groups at the same range of concentrations tested in previous effects and in both experimental groups. These actions were significantly reduced by atropine (10^{-8} M). In addition, the maximal effect of carbachol on PGE_2 production (2.90 ± 0.28 ng·mL^{-1}) was reduced by tropicamide, methoctramine, 4-DAMP and M_3-siRNA in iNIH3T3 cells (Figure 6B), but only by methoctramine in NIH3T3 cells (1.08 ± 0.17 ng·mL^{-1}), thus indicating differences in muscarinic acetylcholine receptor coupling to COX-derived PGE_2 between cells in inflammatory and in non-inflammatory conditions.

LPS plus IFN-γ treatment not only modified the coupling of muscarinic acetylcholine receptors to PGE_2 synthesis, but also up-regulated the expression of COX-2 (P < 0.05), which is the only isoform expressed in these cells (Figure 6C). The latter results were confirmed when cells were pretreated with COX inhibitors, as the addition of NS398, a selective COX-2 inhibitor, was equipotent with indomethacin at blocking carbachol-induced PGE_2 synthesis in both cell groups (Figure 6D).

The participation of the NF-κB pathway in COX-2 function and expression was analysed in the presence of IMD354 in both cell populations. This inhibitor significantly reduced PGE_2 production in both iNIH3T3 and NIH3T3 cells (P < 0.001 or P < 0.01) (Figure 7A). IMD354 also reduced the level of COX-2 expression in both cell populations (P < 0.05) (Figure 7B).

Interactions between NOS and COX are involved in the effects of carbachol

To determine a possible crosstalk mechanism between NOS and COX that could also explain the differences underlying the results described above, carbachol-induced NO production was measured in the presence of COX inhibitors (Figure 8A). Indomethacin and NS398 did not modify carbachol-stimulated NO synthesis in NIH3T3 cells, but they restored NO levels triggered by carbachol to control values in iNIH3T3 cells, indicating that COX-2-derived PGE_2 synthesis did not modulate NOS1 activity in untreated cells, but potentiated NOS activity in iNIH3T3 cells. In contrast, the addition

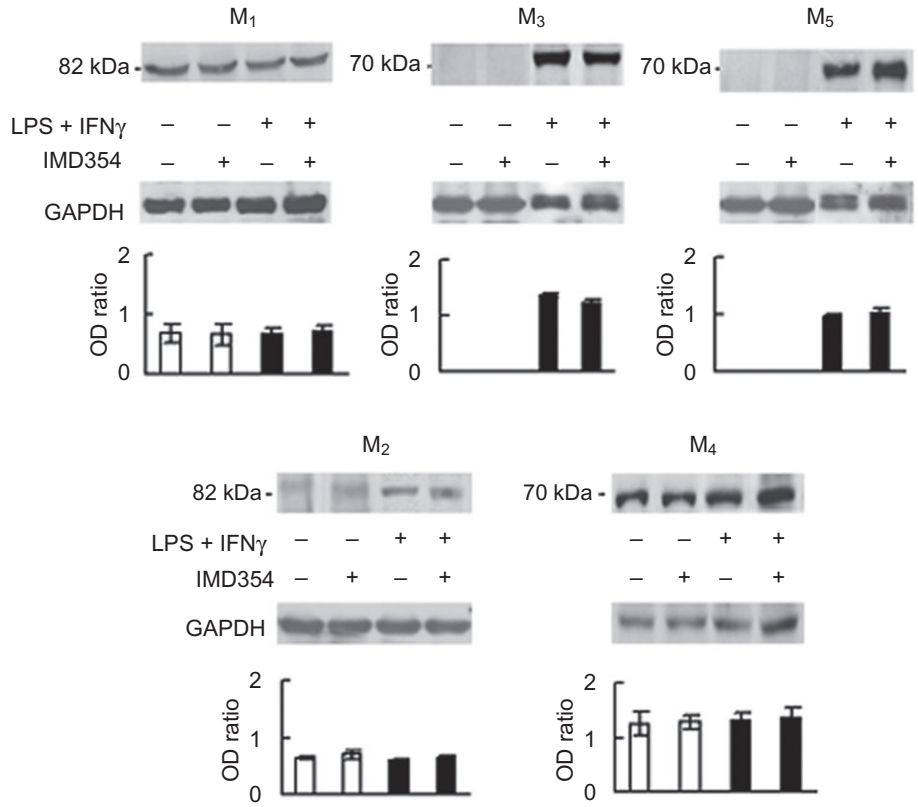

Figure 3

Participation of NF-κB in the expression of muscarinic acetylcholine receptors (M_1–M_5). Cells were cultured in the absence or presence of LPS (10 ng·mL^{-1}) plus IFN-γ (0.5 ng·mL^{-1}) for 72 h without or with IMD354 (10^{-6} M). Molecular weights are on the left. Densitometric analysis of the bands is expressed as optical density (OD) units relative to the expression of GAPDH protein used as loading control. One representative experiment of three is shown.

of A5727 to NIH3T3 cells potentiated the effect of carbachol on PGE_2 synthesis ($P < 0.001$), revealing that NOS1-derived NO could be down-regulating PGE_2 production regulated by COX-2. In iNIH3T3 cells, all NOS inhibitors reduced PGE_2 release ($P < 0.001$ vs. carbachol), indicating that NO derived from NOS1, 2 and 3 stimulates COX-2 activity in inflamed cells (Figure 8B). Moreover, NOS1 is not involved in the proliferative effect triggered by carbachol in NIH3T3 cells, as A5727 was ineffective at reducing this effect of carbachol. Meanwhile, A5727, aminoguanidine and I134 reduced carbachol-induced proliferation in inflamed cells indicating that NO derived from the three isoforms of NOS is the mediator of this effect (Figure 8C). In addition, we confirmed that COX-2-derived products participate in carbachol-induced cell growth, as NS398 inhibited this effect in both NIH3T3 and iNIH3T3 cells (Figure 8D).

Discussion

Our results reveal a novel mechanism involving muscarinic receptors under prolonged inflammatory conditions. The plasticity of these receptors, with regard to their expression and function in murine fibroblasts, could place them at the centre of anti-inflammatory treatment in the future. NIH3T3 cells, which are derived from normal murine fibroblasts, constitute a very useful model to study the role of these stromal cells in the pathophysiology of different processes (Bulseco *et al.*, 2001; Tu-Rapp *et al.*, 2004). The biological activity and proliferative capacity of fibroblasts can either improve or worsen the inflammatory process. Here, we demonstrated that NIH3T3 cells can proliferate in response to the cholinoceptor agonist carbachol, and that this effect was reversed by atropine but not by mecamylamine indicating that only muscarinic acetylcholine receptors are involved in this process. Matthiesen *et al.* (2006) obtained similar results in a primary culture of human lung fibroblasts stimulated with carbachol or oxotremorine.

Our results show that carbachol exerted a more potent effect in LPS plus IFN-γ-treated cells than in untreated cells. This effect was accompanied by the induction of M_3 and M_5 receptor subtypes. It has been documented that LPS can induce the *de novo* synthesis of different types of receptors, such as cytokine receptors (Lattin *et al.*, 2008). In the present study, we showed for the first time that muscarinic acetylcholine receptor protein expression is induced under inflammatory conditions. In addition, we demonstrated that this effect is time-dependent, because short-term stimulation with the same concentrations of LPS and IFN-γ failed to induce the expression of M_3 and M_5 receptors (Español *et al.*, 2010).

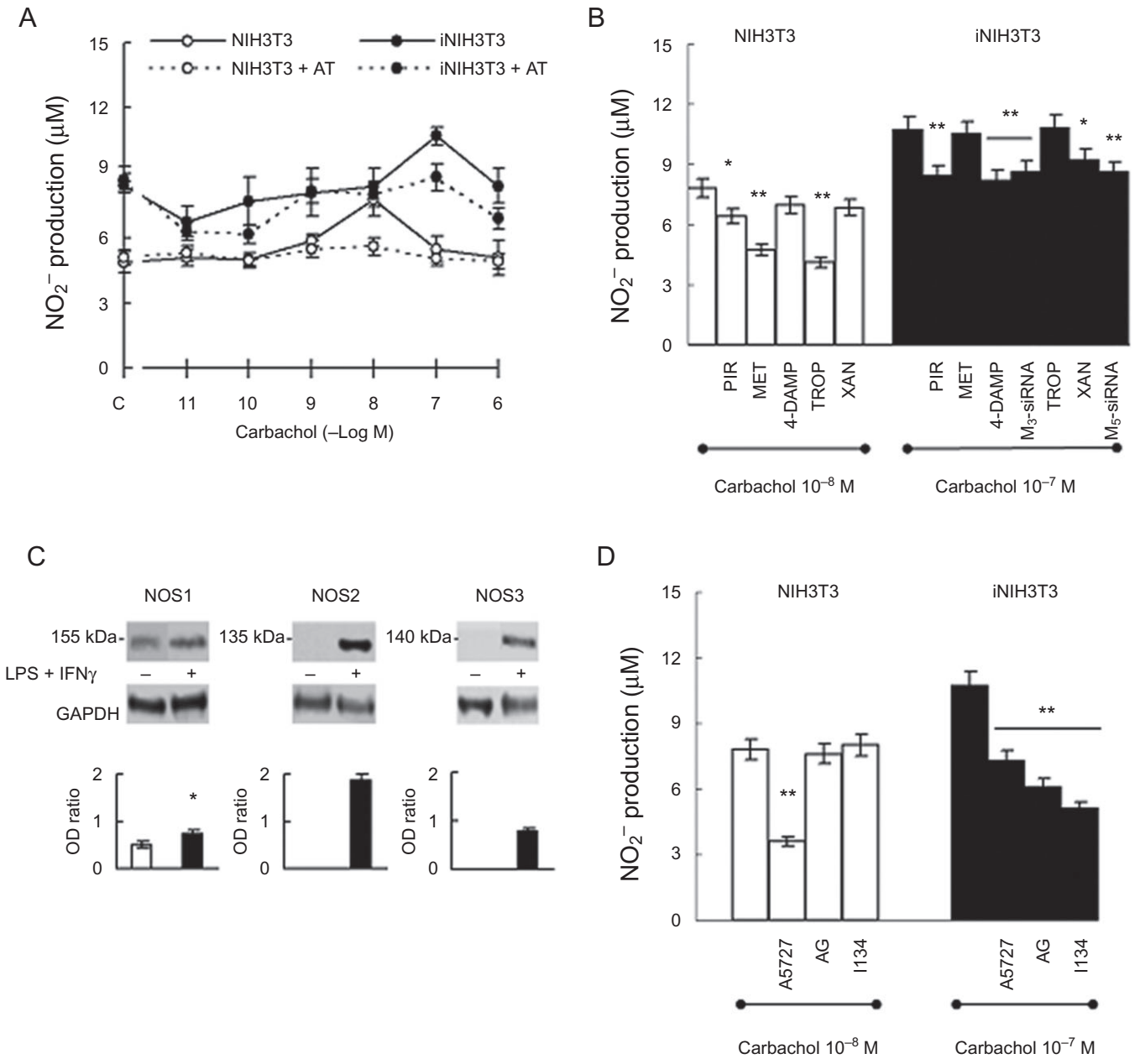

Figure 4

Participation of muscarinic acetylcholine receptors in NOS-derived NO production. (A) Concentration–response curves for the effect of carbachol on NO production. Cells were cultured in the absence or presence of LPS (10 ng·mL^{-1}) plus IFN-γ (0.5 ng·mL^{-1}) for 72 h (NIH3T3 and iNIH3T3, respectively), and then stimulated with different concentrations of carbachol without or with atropine (AT) (10^{-8} M). (B) Effect of the maximal effective concentration of carbachol on NO production in the absence or presence of 10^{-9} M pirenzepine (PIR), methoctramine (MET), 4-DAMP, tropicamide (TROP), xanomeline (XAN) or in iNIH3T3 cells transfected with M_3- or M_5-siRNA. *$P < 0.05$; **$P < 0.001$ versus carbachol. (C) Western blot assay to detect NOS isoforms in untreated or LPS plus IFN-γ-treated cells. Molecular weights are on the left. Densitometric analysis of the bands is expressed as optical density (OD) units relative to the expression of GAPDH protein used as loading control. One representative experiment of three is shown. *$P < 0.05$. (D) Effect of the maximal effective concentration of carbachol on NO production. NIH3T3 and iNIH3T3 cells were treated with carbachol in the absence or presence of A5727 (5×10^{-6} M) aminoguanidine (AG) (10^{-4} M) and I134 (10^{-5} M). Results are expressed as μM concentration of nitrite (NO_2^-) in cell culture supernatants. Values are mean ± SEM of eight experiments performed in triplicate. **$P < 0.001$ versus carbachol.

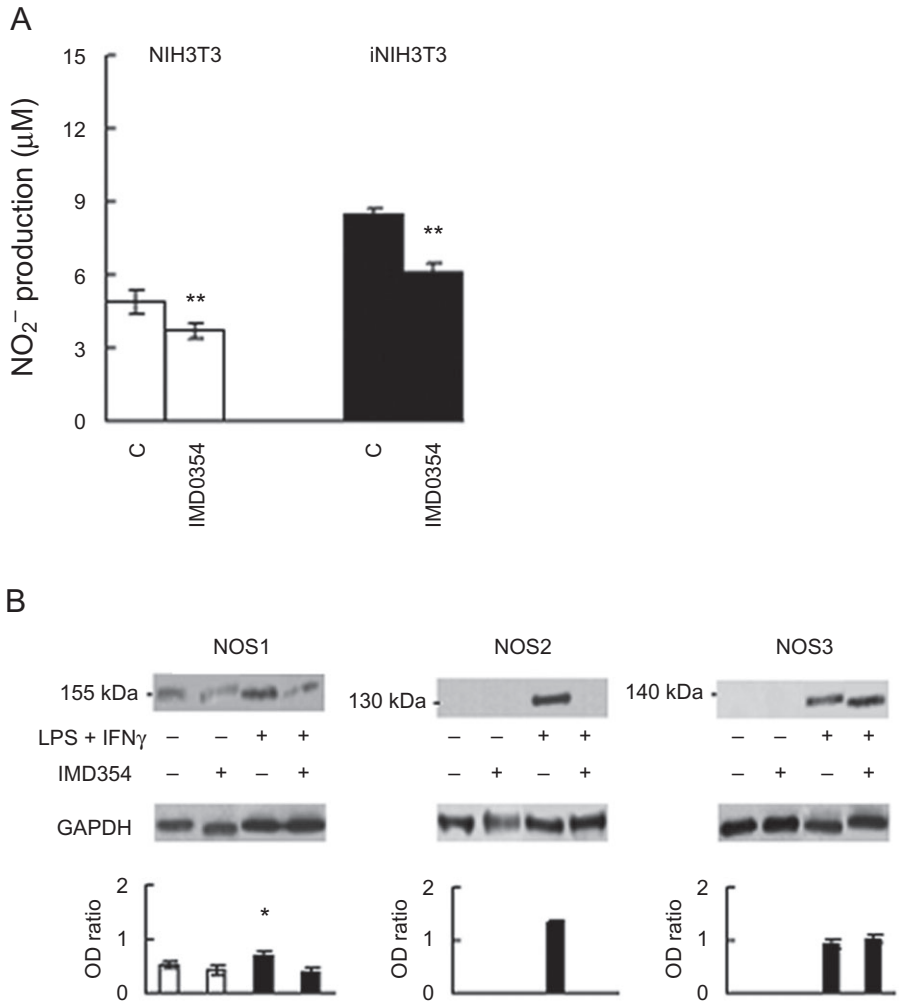

Figure 5

Participation of NF-κB in the activity and expression of NOS. Cells were cultured in the absence or presence of LPS (10 ng·mL^{-1}) plus IFN-γ (0.5 ng·mL^{-1}) for 72 h (NIH3T3 and iNIH3T3, respectively) with or without IMD354 (10^{-6} M). (A) NO production was determined by measuring nitrite (NO_2^-) levels in μM concentration in culture supernatants. Values are mean ± SEM of eight experiments performed in triplicate. $^{**}P < 0.01$ versus control (C). (B) Western blot assays to detect NOS isoforms in untreated or LPS plus IFN-γ-treated cells. Molecular weights are on the left. Densitometric analysis of the bands is expressed as optical density (OD) units relative to the expression of GAPDH protein used as loading control. One representative experiment of three is shown. $^{*}P < 0.05$.

It is well known that different inflammatory stimuli can activate the NF-κB signalling pathway and that this activation can lead to an increase in the expression of several proteins (Bonizzi and Karin, 2004). Although we demonstrated that NF-κB is constitutively active in NIH3T3 cells (Español *et al.*, 2010), our results indicate that this transcription factor is not involved in the *de novo* expression of M_3 and M_5 receptors in these cells.

One of the main effector enzymes in muscarinic acetylcholine receptor transduction pathways is NOS. The enzyme product NO is a central modulator involved in the regulation of several processes, including inflammation, and it is practically accepted that the expression and function of NOS isoenzymes are generally up-regulated in different cell types during this process (Marshall *et al.*, 2000). Here, we observed that LPS plus IFN-γ increased NOS1 expression and induced the *de novo* expression of NOS2 and NOS3 in NIH3T3 cells. de Couto Pita *et al.* (2009) obtained similar results in a model of LPS-induced pulpitis in rats. They observed that the addition of LPS to pulp increased NO production generated by iNOS and also that the muscarinic agonist pilocarpine stimulated iNOS-derived NO synthesis at a similar range of concentrations tested for carbachol in our model. In addition, our results demonstrated collaborative actions among M_1, M_2 and M_4 receptors in both carbachol-stimulated NOS1-derived NO synthesis and in NIH3T3 cell proliferation. Previously, we obtained evidence that M_1 and M_2 receptors have collaborative actions on urea production induced by arginase II and the pro-angiogenic effects exerted by macrophages purified from animals with LMM3 tumours (de la Torre *et al.*, 2005). Inflammatory conditions alter the coupling of NOS to M_1, M_3 and M_5 receptors; activation of these receptors by carbachol

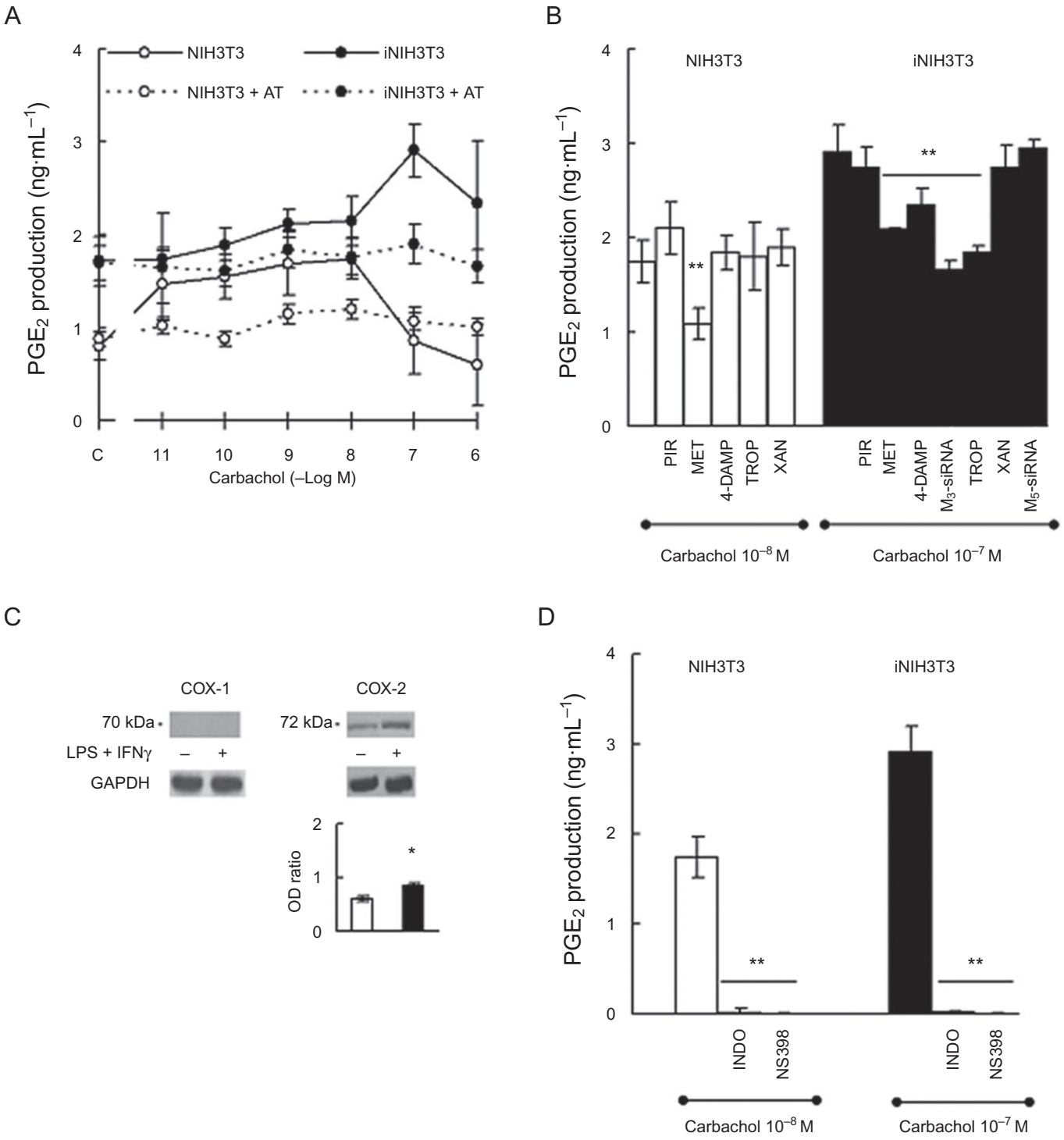

Figure 6

Participation of muscarinic acetylcholine receptors in COX-derived PGE_2 production. (A) Concentration–response curves for effect of carbachol on PGE_2 release. Cells (10^6 per well) were cultured in the absence or presence of LPS (10 ng·mL^{-1}) plus IFN-γ (0.5 ng·mL^{-1}) for 72 h (NIH3T3 and iNIH3T3, respectively), and then stimulated with different concentrations of carbachol without or with atropine (AT) (10^{-8} M). (B) Effect of the maximal effective concentration of carbachol on PGE_2 production in the absence or presence of 10^{-9} M pirenzepine (PIR), methoctramine (MET), 4-DAMP, tropicamide (TROP), xanomeline (XAN) or in iNH3T3 cells transfected with M_3- or M_5-siRNA. $^{**}P < 0.001$ versus carbachol. (C) Western blot assay to detect COX isoforms in untreated or LPS plus IFN-γ-treated cells. Molecular weights are on the left. Densitometric analysis of the bands is expressed as optical density (OD) units relative to the expression of GAPDH protein used as loading control. One representative experiment of three is shown. $^{*}P < 0.05$. (D) Effect of carbachol on PGE_2 production. NIH3T3 and iNIH3T3 cells were treated with carbachol in the absence or presence of indomethacin (INDO) (10^{-6} M) or NS398 (10^{-5} M). Results are expressed as ng·mL^{-1} of liberated PGE_2. Values are mean ± SEM of six experiments performed in duplicate. $^{**}P < 0.001$ versus carbachol.

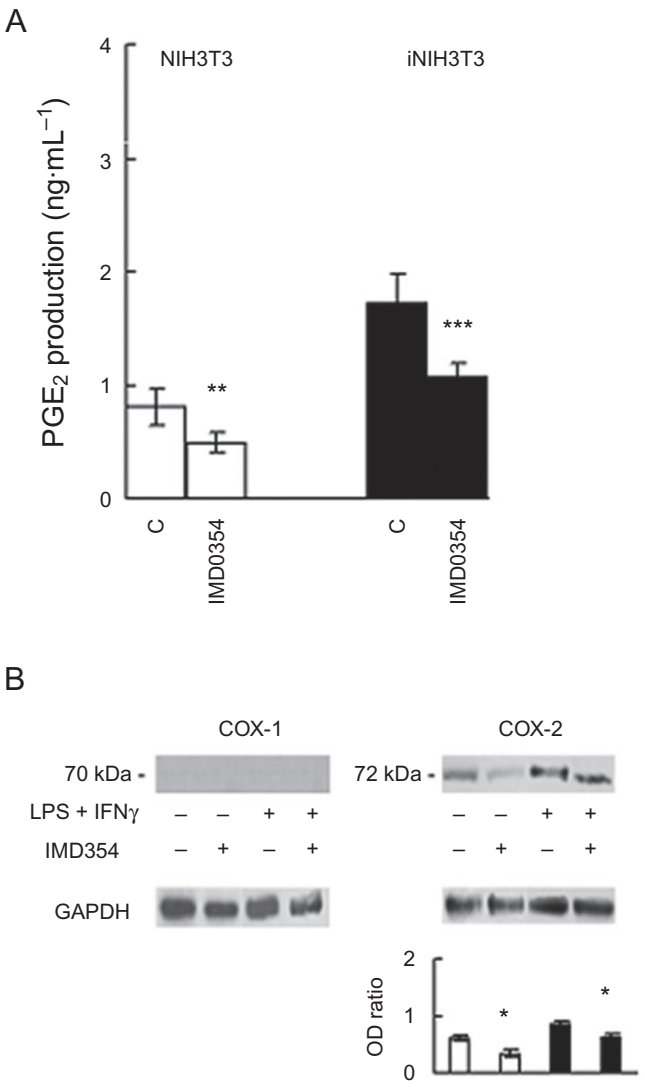

Figure 7

Participation of NF-κB in the activity and expression of COX. Cells were cultured in the absence or presence of LPS (10 ng·mL^{-1}) plus IFN-γ (0.5 ng·mL^{-1}) for 72 h (NIH3T3 and iNIH3T3, respectively) without or with IMD354 (10^{-6} M). (A) PGE_2 production in culture supernatants was determined by radioimmunoassay and expressed in ng·mL^{-1}. Values are mean ± SEM of six experiments performed in duplicate. $^{**}P < 0.01$ and $^{***}P < 0.001$ versus control (C). (B) Western blot assays to detect COX isoforms in untreated or LPS plus IFN-γ-treated cells. Molecular weights are on the left. Densitometric analysis of the bands is expressed as optical density (OD) units relative to the expression of GAPDH protein used as loading control. One representative experiment of three is shown. $^{*}P < 0.05$.

stimulates NO production via the coupling of $G_{q/11}$ protein to PLC, an event that has been associated with the proliferation of different cell types (Eglen, 2006; Kaproth-Joslin *et al.*, 2008). Fan *et al.* (2011) demonstrated that the administration of LPS induces the inactivation of Giα protein in RAW264.6 cells mediated by toll-like receptors in an endotoxaemia model before the death of animals as a result of septic shock. A similar mechanism may be involved in our model in which M_2 and M_4 receptors, which are generally linked to Gi protein, switched their coupling from NO production in NIH3T3 cells to PGE_2 synthesis after flogogen treatment. The latter could be due to the stimulation of PLA_2 via Giβγ protein by a different activation pathway as previously reported by Selbie and Hill (1998).

Another main effector enzyme in muscarinic acetylcholine receptor signalling pathways is COX. We demonstrated that inflammatory stimuli increase both COX-2 expression and PGE_2 production mediated by NF-κB activation. Pausawasdi *et al.* (2002) reported that COX-2 expression and function are induced by LPS treatment *in vitro* via the NF-κB pathway. In addition, Matsuura *et al.* (1999) demonstrated that IFN-γ treatment of human keratinocytes increases PGE_2 levels, which could positively modulate cell proliferation. Felder (1995) reported that M_2 receptors can also couple to PLA_2 and stimulate arachidonic acid release from the plasma membrane. This may be the case in NIH3T3 cells because only the M_2 selective antagonist methoctramine reduced carbachol-induced PGE_2 release. The presence of inflammatory stimuli increased the ability of M_3 and M_4 receptor activation to release PGE_2. The latter could be related to previous observations describing a down-regulation of M_2 receptor function during the inflammatory process produced by virus infections. Fryer *et al.* (1990) attributed these results to the action of viral neuraminidase, which cleaves sialic acid residues, decreasing the affinity of agonists for these receptors.

Several studies have demonstrated that NOS and COX can reciprocally modulate their activities and thus the response of cells in different conditions (Nogawa *et al.*, 1998; Salvemini *et al.*, 2013). Our results indicate that COX-2 products are unable to modulate NO synthesis in NIH3T3 cells but can stimulate NO synthesis in iNIH3T3 cells. However, in untreated cells, NOS1-derived NO inhibited COX-2 activity, as A5727 potentiated PGE_2 release, while in iNIH3T3 cells NO stimulated PGE_2 production, thus revealing a positive feedback mechanism between NOS and COX in inflamed cells. The negative regulation observed between NOS and COX in non-inflamed cells would be responsible for the lack of involvement of NOS1 in the proliferative effect of carbachol and for a negative control on cell proliferation in the absence of inflammation.

Our results show, for the first time, that inflammation induces the expression of muscarinic acetylcholine receptors in murine fibroblasts, increasing the ability of carbachol to stimulate cell proliferation. Treatment with LPS plus IFN-γ induced the expression of NOS1, NOS2, NOS3 and COX2, so potentiating the effect of carbachol on NO and PGE_2 production. Inflammation evokes a positive crosstalk mechanism between NOS and COX to be triggered by carbachol, indicating the potential of muscarinic acetylcholine receptors as therapeutic targets in inflammation.

Acknowledgements

We want to thank Mrs María E. Castro and Ana I. Casella for their excellent technical assistance. Alejandro Español, María Gabriela Lombardi and Maria Elena Sales are established investigators from the National Research Council (CONICET) Paola Martínez Pulido is a fellow of CONICET. We also want

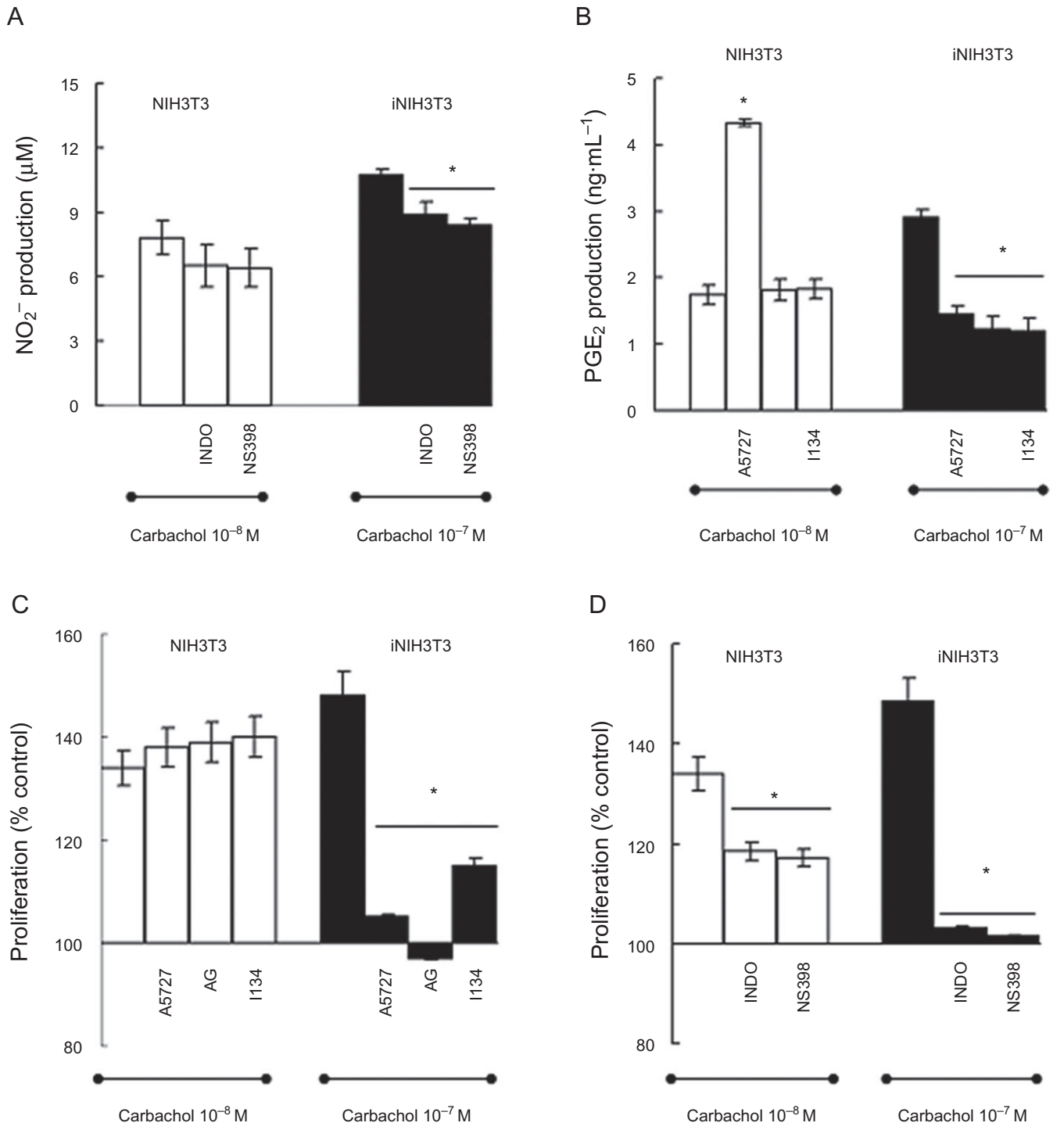

Figure 8

Crosstalk interactions between NOS and COX. Cells were cultured in the absence or presence of LPS (10 ng·mL^{-1}) plus IFN-γ (0.5 ng·mL^{-1}) for 72 h (NIH3T3 and iNIH3T3, respectively) and then stimulated with carbachol. (A) NO production was quantified by measuring nitrite (NO_2^-) concentration in μM in culture supernatants in the absence or presence of indomethacin (INDO) (10^{-6} M) or NS398 (10^{-5} M) in eight experiments performed in triplicate. (B) PGE_2 production was measured by radioimmunoassay in the absence or presence of NOS inhibitors: A5727 (5×10^{-6} M), aminoguanidine (AG) (10^{-4} M) or I134 (10^{-5} M). Results are expressed in ng·mL^{-1} ($n = 6$). (C) NOS participation in cell proliferation measured as % change with respect to control (considered as 100%). NIH3T3 and iNIH3T3 cells were treated with carbachol in the absence or presence of NOS inhibitors: A5727 (5×10^{-6} M), AG (10^{-4} M) or I134 (10^{-5} M) ($n = 6$). (D) NIH3T3 and iNIH3T3 cells were treated with carbachol in the absence or presence of COX inhibitors: indomethacin (INDO) (10^{-6} M) or NS398 (10^{-5} M) ($n = 6$). Values are mean ± SEM. *$P < 0.001$ versus carbachol.

to thank the University of Buenos Aires for the grant UBACYT 2011-2014 200201100100012 and the National Research Council for the grant PIP 2010-2012 11420090007901.

Author contributions

A. E. and M. M. performed proliferation experiments, nitric oxide synthase activity and expression assays, and statistical analysis; M. C. performed PGE_2 radioimmunoassay; P. M. P. and M. G. L. performed siRNA designing and transfections and Western blot for muscarinic receptor detection; M. E. S. performed analysis of results and paper writing.

Conflict of interest

None.

References

Alexander SPH, Benson HE, Faccenda E, Pawson AJ, Sharman JL, Spedding M *et al*. (2013a). The Concise Guide to PHARMACOLOGY 2013/14: G protein-coupled receptors. Br J Pharmacol 170: 1459–1581.

Alexander SPH, Benson HE, Faccenda E, Pawson AJ, Sharman JL, Spedding M *et al*. (2013b). The Concise Guide to PHARMACOLOGY 2013/14:Ligand-gated ion channels. Br J Pharmacol 170: 1582–1603.

Alexander SPH, Benson HE, Faccenda E, Pawson AJ, Sharman JL, Spedding M *et al*. (2013c). The Concise Guide to PHARMACOLOGY 2013/14: Catalytic receptors. Br J Pharmacol 170: 1676–1703.

Alexander SPH, Benson HE, Faccenda E, Pawson AJ, Sharman JL, Spedding M *et al*. (2013d). The Concise Guide to PHARMACOLOGY 2013/14:Enzymes. Br J Pharmacol 170: 1797–1862.

Bonizzi G, Karin M (2004). The two NF-kappa B activation pathways and their role in innate and adaptive immunity. Trends Immunol 25: 280–288.

Bradford MM (1976). A rapid and sensitive method for the quantification of microgram quantities of protein utilizing the principle of protein-dye binding. Anal Biochem 72: 248–254.

Buckley CD (2003). Why does chronic inflammatory joint disease persist? Clin Med 3: 361–366.

Bulseco DA, Poluha W, Schonhoff CM, Daou MC, Condon PJ, Ross AH (2001). Cell-cycle arrest in TrkA-expressing NIH 3T3 involves nitric oxide synthase. J Cell Biochem 81: 193–204.

Chen TR (1977). In situ detection of mycoplasma contamination in cell cultures by fluorescent Hoescht 33258 stain. Exp Cell Res 104: 255–262.

de Couto Pita A, Passafaro D, Ganzinelli S, Borda E, Sterin-Borda L (2009). Differential cholinoceptor modulation of nitric oxide isoforms in experimentally-induced inflammation of dental pulp tissue. Int Endod J 42: 525–533.

Eglen RM (2006). Muscarinic receptor subtypes in neuronal and non-neuronal cholinergic function. Auton Autacoid Pharmacol 26: 219–233.

Eglen RM (2012). Overview of muscarinic receptor subtypes. Handb Exp Pharmacol 208: 3–28.

Español AJ, Sales ME (2004). Different muscarinic receptors are involved in the proliferation of murine mammary adenocarcinoma cell lines. Int J Mol Med 13: 311–317.

Español AJ, de la Torre E, Fiszman GL, Sales ME (2007). Role of non-neuronal cholinergic system in breast cancer progression. Life Sci 80: 2281–2285.

Español AJ, Goren N, Ribeiro ML, Sales ME (2010). Nitric oxide synthase 1 and cyclooxygenase-2 enzymes are targets of muscarinic activation in normal and inflamed NIH3T3 cells. Inflamm Res 59: 227–238.

Fan H, Li P, Zingarelli B, Borg K, Halushka PV, Birnbaumer L *et al*. (2011). Heterotrimeric Gα(i) proteins are regulated by lipopolysaccharide and are anti-inflammatory in endotoxemia and polymicrobial sepsis. Biochim Biophys Acta 1813: 466–472.

Felder CC (1995). Muscarinic acetylcholine receptors: signal transduction through multiple effectors. FASEB J 9: 619–625.

Fiszman G, Cattaneo V, de la Torre E, Español A, Colombo L, Sacerdote de Lustig E *et al*. (2006). Muscarinic receptors autoantibodies purified from mammary adenocarcinoma-bearing mice sera stimulate tumor progression. Int Immunopharmacol 6: 1323–1330.

Forsgren S, Grimsholm O, Jönsson M, Alfredson H, Danielson P (2009). New insight into the non-neuronal cholinergic system via studies on chronically painful tendons and inflammatory situations. Life Sci 84: 865–870.

Fryer AD, el Fakahany EE, Jacoby DB (1990). Parainfluenza virus type 1 reduces the affinity of agonists for muscarinic receptors in guinea-pig lung and heart. Eur J Pharmacol 181: 51–58.

Granstrom E, Kindhal H (1978). Radioimmunoassay of prostaglandins and thromboxanes. Adv Prostaglandin Thromboxane Res 5: 119–210.

Kaproth-Joslin KA, Li X, Reks SE, Kelley GG (2008). Phospholipase C delta 1 regulates cell proliferation and cell-cycle progression from G1- to S-phase by control of cyclin E-CDK2 activity. Biochem J 415: 439–448.

Kohn EC, Alessandro R, Probst J, Jacobs W, Brilley E, Felder CC (1996). Identification and molecular characterization of a m5 muscarinic receptor in A2058 human melanoma cells. Coupling to inhibition of adenylyl cyclase and stimulation of phospholipase A2. J Biol Chem 271: 17476–17484.

Kumar P, Chakrabarti I (2009). Idiopathic carpal tunnel syndrome and trigger finger: is there an association? J Hand Surg Eur 34: 58–59.

Lattin JE, Schroder K, Su AI, Walker JR, Zhang J, Wiltshire T *et al*. (2008). Expression analysis of G protein-coupled receptors in mouse macrophages. Immunome Res 29: 4–5.

Marshall H, Merchant K, Stamler J (2000). Nitrosation and oxidation in the regulation of gene expression. FASEB J 14: 1889–1900.

Matsuura H, Sakaue M, Subbaramaiah K, Kamitani H, Eling TE, Dannenberg AJ *et al*. (1999). Regulation of cyclooxygenase-2 by interferon gamma and transforming growth factor α in normal human epidermal keratinocytes and squamous carcinoma cells. Role of mitogen-activated protein kinases. J Biol Chem 274: 29138–29148.

Matthiesen S, Bahulayan A, Kempkens S, Haag S, Fuhrmann M, Stichnote C *et al*. (2006). Muscarinic receptors mediate stimulation

of human lung fibroblast proliferation. Am J Respir Cell Mol Biol 35: 621–627.

Nogawa S, Forster C, Zhang F, Nagayama M, Ross ME, Iadecola C (1998). Interaction between inducible nitric oxide synthase and cyclooxygenase-2 after cerebral ischemia. Proc Natl Acad Sci USA 95: 10966–10971.

Pausawasdi N, Ramamoorthy S, Crofford LJ, Askari FK, Todisco A (2002). Regulation and function of COX-2 gene expression in isolated gastric parietal cells. Am J Physiol Gastrointest Liver Physiol 282: G1069–G1078.

Pawson AJ, Sharman JL, Benson HE, Faccenda E, Alexander SP, Buneman OP *et al.*; NC-IUPHAR (2014). The IUPHAR/BPS Guide to PHARMACOLOGY: an expert-driven knowledgebase of drug targets and their ligands. Nucl Acids Res 42 (Database Issue): D1098–106.

Salvemini D, Kim SF, Mollace V (2013). Reciprocal regulation of the nitric oxide and cyclooxygenase pathway in pathophysiology: relevance and clinical implications. Am J Physiol Regul Integr Comp Physiol 304: R473–R487.

Selbie LA, Hill SJ (1998). Selbie G protein-coupled-receptor cross-talk: the fine-tuning of multiple receptor-signalling pathways. Trends Pharmacol Sci 19: 87–93.

Spang C, Alfredson H, Ferguson M, Roos B, Bagge J, Forsgren S (2013). The plantaris tendon in association with mid-portion Achilles tendinosis – tendinosis-like morphological features and presence of a non-neuronal cholinergic system. Histol Histopathol 8: 623–632.

de la Torre E, Davel L, Jasnis MA, Gotoh T, de Lustig ES, Sales ME (2005). Muscarinic receptors participation in angiogenic response induced by macrophages from mammary adenocarcinoma-bearing mice. Breast Cancer Res 7: R345–R352.

Tu-Rapp H, Hammermüller A, Mix E, Kreutzer HJ, Goerlich R, Köhler H *et al.* (2004). A proinflammatory role for Fas in joints of mice with collagen-induced arthritis. Arthritis Res Ther 6: R404–R414.